MIKAILALSYS
Journal of Multidisciplinary Sciences

e-ISSN : 2987-2286
p-ISSN : 2987-3924
Index: Harvard, Boston, Sydney, Copernicus, Sinta 4, Scilit, Semantic, Google, etc

https://doi.org/10.58578/mikailalsys.v4i3.12177

Application of Geographic Information Systems (GIS) for Analyzing Residential Damage Caused by Cold Lahar Floods in Sungai Pua and Canduang Districts

Muhamat Danil & Triyatno
Universitas Negeri Padang
muhamatdanil13@gmail.com

Submitted:	Revised:	Accepted:	Published:
Aug 10, 2026	Sep 7, 2026	Sep 19, 2026	Sep 24, 2026

Abstract

Cold lahar floods originating from Mount Marapi have caused substantial landscape changes and residential damage, underscoring the need for reliable spatial information to support post-disaster management. Although previous research has primarily addressed hazard mapping and affected-area delineation, integrated assessments combining change detection with spatial analysis of residential damage remain limited. This study analyzed the extent and spatial pattern of residential damage in Sungai Pua and Canduang Districts. A descriptive quantitative approach integrating geographic information systems (GIS) and remote sensing was employed. Pre- and post-disaster Sentinel-2 imagery was analyzed using the Normalized Difference Vegetation Index (NDVI), Normalized Difference Built-up Index (NDBI), Maximum Likelihood Classification, Post-Classification Comparison, and Ripley's K-function. The analysis was supported by field verification of 114 affected buildings. The ΔNDVI-based affected areas accounted for 66.3% of Sungai Pua and 54.9% of Bukik Batabuah. Field observations identified 64 lightly damaged, nine moderately damaged, and 41 severely damaged buildings. Residential damage in Sungai Pua exhibited a significant clustered pattern across distances of 60–600 m, whereas Bukik Batabuah generally displayed a random pattern with localized clustering at 50 m. These findings demonstrate that integrating GIS, multitemporal satellite imagery, spatial point-pattern analysis, and field verification provides a robust approach to post-disaster residential damage assessment. This integrated framework can support targeted recovery measures and risk-sensitive settlement planning in areas exposed to future lahar floods.

Keywords: Change Detection; Cold Lahar Floods; Geographic Information Systems; Residential Damage; Ripley's K-Function

INTRODUCTION

Indonesia is situated within one of the world's most active volcanic regions, where interactions among major tectonic plates have formed an extensive chain of volcanoes across the archipelago. The Indonesian Ministry of Energy and Mineral Resources reported that the country has 127 active volcanoes, accounting for approximately 13% of the world's active volcanoes, while millions of people live in areas exposed to volcanic hazards (Ministry of Energy and Mineral Resources (Agam, 2024). This geological setting creates persistent risks not only from primary volcanic processes, such as eruptions, ashfall, pyroclastic material, and volcanic gases, but also from secondary hazards that may continue after an eruption has subsided. Hermon (2015) emphasizes that volcanic disaster risk in Indonesia is closely related to the interaction between physical hazards, exposed populations, land use, and the capacity of communities to respond to hazardous events. Such conditions make post-eruption hazards particularly important in densely inhabited areas surrounding active volcanoes.

Rain-triggered lahars, commonly referred to in Indonesia as *cold lahar floods*, are among the most destructive secondary volcanic hazards. Lahars develop when loose volcanic deposits, including ash, sand, gravel, and larger rock fragments, are remobilized by water and transported downslope through river channels and valleys. Their destructive capacity differs from that of ordinary flooding because the flow carries a substantial sediment load and coarse volcanic material that can generate intense impact, abrasion, burial, and structural failure. Observations of rain-triggered lahars have shown that variations in sediment concentration, flow velocity, channel conditions, and rainfall can strongly influence their destructive power (Ramos et al., 2024). Long-term hazard assessments also demonstrate that lahar processes can remain relevant well beyond the eruptive phase because volcanic deposits may be repeatedly remobilized during intense rainfall (Tierz et al., 2024). Residential areas located along drainage networks are consequently exposed not only to inundation but also to direct physical damage to buildings, roads, bridges, agricultural land, and other elements of community life (Wulansari et al., 2024).

Mount Marapi in West Sumatra illustrates the continuing interaction between volcanic activity, rainfall, river systems, and human settlements. The rain-triggered lahar and flash-flood disaster of 11 May 2024 caused widespread casualties and physical damage across several areas of West Sumatra, particularly Agam and Tanah Datar Regencies. Official emergency assessments documented extensive damage to settlements and public infrastructure, while casualty figures continued to change as search and rescue operations progressed(BPBD Agam, 2024). An early BNPB assessment in Agam Regency recorded 193 affected houses, including houses classified as lightly and severely damaged, together with extensive impacts on agricultural land and community infrastructure. Subsequent updates continued to record deaths and missing persons, illustrating both the magnitude of the event and the challenges faced during post-disaster assessment. The consequences extended beyond damaged structures, as affected households also faced disruption to mobility, access to services, livelihoods, and the security of their living environment.

Sungai Pua and Canduang Districts were among the areas directly affected by the May 2024 disaster in Agam Regency. Both districts contain settlements associated with drainage systems originating from the slopes of Mount Marapi, creating significant exposure when rainfall remobilizes volcanic deposits into river channels. BNPB identified Sungai Pua and Canduang among the affected districts during the emergency response, with fatalities, damaged settlements, and evacuations reported across the affected areas (BNPB, 2024). Recent studies around Mount Marapi have similarly demonstrated the spatial importance of river corridors, settlement location, and land use in understanding lahar-related impacts.Sari et al (2025), for example, mapped areas affected by the Mount Marapi cold lahar using Sentinel-2 imagery in Sungai Pua, while Wulandari et al. (2025) examined evacuation locations as part of lahar-flood mitigation on the southern side of Mount Marapi. These findings indicate that spatial information is essential for understanding not only where a disaster occurs but also how its consequences are distributed across inhabited landscapes.

Post-disaster assessment requires information that can be produced rapidly while retaining sufficient spatial detail to distinguish the extent and location of damage. Conventional field surveys remain important because they provide direct observations of structural conditions, yet their implementation can be constrained by inaccessible roads, unstable terrain, debris accumulation, and the wide geographical extent of affected areas. Remote sensing and Geographic Information Systems (GIS) provide a complementary approach by enabling observations from multiple dates to be organized, compared, quantified, and represented spatially. Ahmed et al. (2024), in their review of post-disaster building damage assessment, highlight the growing role of satellite imagery and computational techniques in supporting damage identification and disaster response. Braik & Koliou (2024) likewise demonstrate that the integration of satellite imagery and GIS can support large-scale building damage mapping and reveal spatial variations that may be difficult to identify through field assessment alone. These capabilities are particularly relevant in volcanic environments where damaged settlements may be dispersed along several river corridors.

Change detection provides a practical analytical framework for identifying physical transformations by comparing remotely sensed information acquired at different times. The approach can reveal changes between pre-disaster and post-disaster conditions and translate those differences into spatial information that supports interpretation of affected areas. Goswami et al. (2022) showed that remote-sensing change detection can be performed through both algebraic and machine-learning approaches, whereas Zakeri et al. (2019) demonstrated the value of combining change-vector analysis with post-classification comparison for multispectral data. More recent developments have introduced difference-aware attention and refined image-comparison techniques to improve sensitivity to spatial changes in satellite imagery (Azizah & Irawan, 2023; Mei et al., 2023). Indonesian studies have also applied multi-temporal satellite data to flood environments, including Sentinel-1 SAR-based mapping by Budiarto & Bioresita (2023) and (K. Y. Sari & Triyatno, 2024). Collectively, these studies show that change detection is not merely an image-comparison procedure; when integrated within GIS, it can provide a spatial basis for distinguishing affected locations and interpreting the geographical distribution of disaster impacts.

Research on volcanic and lahar-related hazards in Indonesia has developed along several complementary directions, although the emphasis has varied considerably. Azizah & Irawan (2023) used geospatial techniques to detect changes in lahar channels following the 2021 Semeru eruption, demonstrating the usefulness of multi-temporal analysis for tracing post-eruption landscape change. In the Mount Marapi region, Aisy & Hermon (2024) examined cold-lahar hazard and risk in Tanah Datar Regency using GIS-based scoring and overlay techniques, while Yanto et al. (2024) investigated damage to settlement land in areas affected by the Mount Marapi lahar disaster. Sari et al. (2025) subsequently mapped lahar-affected areas in Sungai Pua using Sentinel-2 satellite imagery, and Wulandari et al. (2025) focused on community evacuation locations for lahar-flood mitigation. These studies have contributed important evidence concerning hazard levels, affected land, evacuation, and the wider spatial consequences of the Mount Marapi disaster.

A closer reading of the previous studies indicates that detailed spatial assessment of residential damage across Sungai Pua and Canduang as two connected but distinct affected districts remains comparatively limited. Existing work around Mount Marapi has largely addressed hazard and risk zoning, affected-area mapping, settlement-land impacts, or evacuation planning (Aisy & Hermon, 2025; Sari et al., 2025; Wulandari et al., 2025; Yanto et al., 2024). Research applying *change detection* elsewhere has established its value for identifying disaster-induced physical changes, yet the approach still needs to be contextualized to local settlement conditions and the spatial characteristics of rain-triggered lahar impacts (Goswami et al., 2022; Zakeri et al., 2019). The present study addresses this space by combining GIS-based *change detection* with an analysis of the spatial distribution of damaged residential areas in both Sungai Pua and Canduang. The contribution lies in shifting the analytical focus from identifying a broadly affected zone toward examining how residential damage itself is distributed across two highly exposed districts, thereby providing more location-specific information for post-disaster assessment and risk-sensitive settlement planning.

The study therefore aims to apply Geographic Information Systems (GIS) to identify, map, and analyze residential damage caused by the Mount Marapi cold lahar flood in Sungai Pua and Canduang Districts, Agam Regency. The analysis focuses on detecting changes in residential areas through a *change detection* approach and examining the spatial distribution of the resulting damage. The study is expected to provide geographically explicit evidence that can support post-disaster assessment, recovery priorities, and future disaster-risk-informed planning in settlements exposed to rain-triggered lahar hazards.

METHODS

This study employed a descriptive quantitative approach with a spatial analytical design, integrating Geographic Information Systems (GIS) and remote sensing to assess residential damage caused by the Mount Marapi cold lahar flood. A quantitative approach was considered appropriate because the analysis relied on measurable spatial and spectral variables, including pre- and post-disaster NDVI and NDBI values, land-cover change, and the spatial distribution of damaged buildings. The study was conducted in Nagari Sungai Pua, Sungai Pua District, and Nagari Bukik Batabuah, Canduang District, Agam Regency, West Sumatra. The population consisted of all residential buildings identified as affected by the disaster, comprising 65 buildings in Sungai Pua and 49 buildings in Canduang. Following Nazir's (2005) concept of population and sampling, all 114 affected residential buildings were included through or a census approach. This strategy was selected because the population was relatively manageable and allowed the analysis to represent the entire set of documented affected buildings rather than relying on a subset.

The study used both primary and secondary data. Primary data were obtained through field observations, *ground checks*, geographic coordinate recording, visual documentation of damaged buildings, and in-depth interviews with affected residents and relevant local institutions. Coordinate points of damaged buildings were recorded using GPS-based mapping applications, including UTM Geo Map, to support spatial verification. Secondary data consisted of pre- and post-disaster Sentinel-2 satellite imagery, Digital Elevation Model Nasional (DEMNAS) data, administrative boundary shapefiles, and river-network data obtained from relevant geospatial and government sources. The satellite imagery was subjected to geometric and atmospheric correction, clipping according to the study-area boundaries, and coordinate-system adjustment before analysis. Field observations served as an important validation step for interpreting satellite-derived changes and confirming the actual condition of affected residential buildings. Because the study did not employ a psychometric questionnaire or scale, conventional questionnaire validity and reliability testing was not applicable; spatial interpretation was instead verified through field-based observations and coordinate matching.

Data analysis was conducted through a sequence of spectral, change-detection, damage-classification, and spatial-pattern analyses. NDVI and NDBI were calculated from the Sentinel-2 imagery to identify changes in vegetation and built-up characteristics before and after the disaster, followed by calculation of ΔNDVI and ΔNDBI to quantify spectral changes. Pre- and post-disaster images were then independently classified using supervised Maximum Likelihood Classification (MLC) into built-up areas, vegetation, water bodies, open land or volcanic material, and agricultural land. A Post-Classification Comparison (PCC) procedure was subsequently applied to identify land-cover changes associated with the lahar event. Residential damage was categorized into light, moderate, and severe levels by combining changes in NDVI, NDBI, and land-cover classes, following the change-detection-based damage assessment framework adopted from Sari and Triyatno (2024). The spatial distribution of damaged buildings was further examined using Multi-Distance Spatial Cluster Analysis (Ripley's K-function) in ArcGIS. This method evaluates spatial dependence across multiple distance bands and identifies whether damaged buildings tend to form clustered or dispersed patterns; an observed K-value greater than the expected K-value indicates clustering, whereas a lower observed value indicates spatial dispersion (Self et al., 2023).

RESULTS

1. Topographic Characteristics of the Study Area

Slope analysis was conducted to describe the topographic setting of Sungai Pua and Bukik Batabuah and its relationship with the pathways through which volcanic material can move from the upper slopes of Mount Marapi toward inhabited areas. Five slope classes were identified: flat (0–8%), gentle (8–15%), moderately steep (15–25%), steep (25–45%), and very steep (>45%). Figure 1, Slope Map of Sungai Pua and Bukik Batabuah, shows that steep and very steep terrain is concentrated toward the upper part of the study area, whereas flatter terrain occurs predominantly at lower elevations where settlements and agricultural activities are more developed.

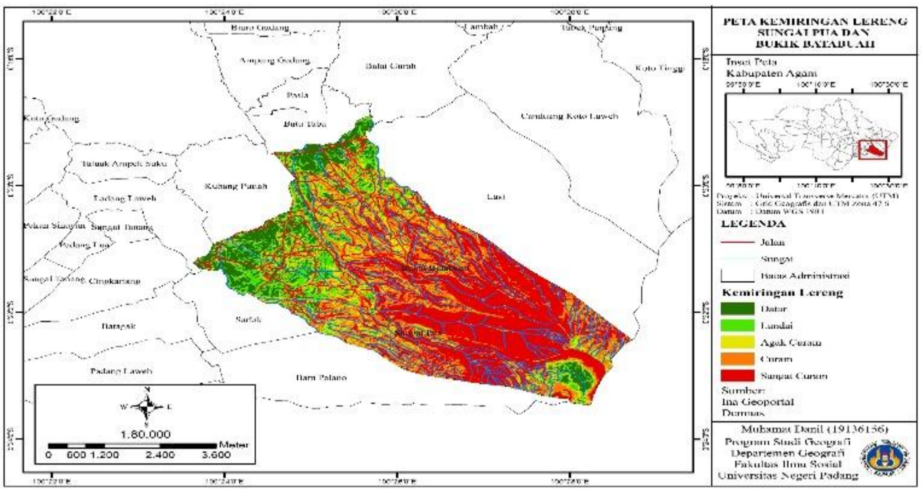

Figure 1. Slope Map of Sungai Pua and Bukik Batabuah

The distribution of slope classes is summarized in Table 1. Very steep slopes constituted the largest class in both study areas, covering 419.26 ha (28.5%) in Sungai Pua and 835.97 ha (42.5%) in Bukik Batabuah. Steep slopes accounted for an additional 291.28

ha (19.8%) and 518.22 ha (26.3%), respectively. Taken together, steep and very steep terrain represented almost half of Sungai Pua and more than two-thirds of Bukik Batabuah. These results demonstrate the strong topographic influence of the Mount Marapi volcanic landscape on both study areas.

Table 1. Slope Classification of Sungai Pua and Bukik Batabuah

Slope class	Slope (%)	Sungai Pua (ha)	Sungai Pua (%)	Bukik Batabuah (ha)	Bukik Batabuah (%)
Flat	0–8	261.38	17.8	157.09	8.0
Gentle	8–15	276.28	18.8	185.61	9.5
Moderately steep	15–25	222.12	15.1	269.20	13.7
Steep	25–45	291.28	19.8	518.22	26.3
Very steep	>45	419.26	28.5	835.97	42.5
Total	—	1,470.32	100.0	1,966.09	100.0

Source: DEMNAS data processing, 2026.

2. Changes in Spectral Indices Before and After the Disaster

a. NDVI Changes

The *Normalized Difference Vegetation Index* (NDVI) was used to identify changes in vegetation conditions between the pre-disaster and post-disaster periods. The analysis revealed a marked reduction in the high-vegetation class in both study areas, accompanied by expansion of non-vegetated and lower-density vegetation classes. The changes were considerably more pronounced in Sungai Pua.

As presented in Table 2**,** high vegetation in Sungai Pua declined from 799.02 ha before the disaster to 575.90 ha after the disaster, representing a reduction of 223.12 ha or 15.2% of the study area. At the same time, non-vegetated land increased by 29.77 ha, very low vegetation by 36.04 ha, low vegetation by 83.39 ha, and moderate vegetation by 73.92 ha. The total area experiencing a change in NDVI class reached 446.24 ha, equivalent to 30.4% of Sungai Pua.

Bukik Batabuah exhibited a similar but less extensive pattern. High vegetation decreased from 1,465.01 ha to 1,343.58 ha, corresponding to a reduction of 121.43 ha or 6.2% of the total area. Moderate vegetation increased by 65.99 ha, low vegetation by 34.68 ha, very low vegetation by 14.04 ha, and non-vegetated land by 6.76 ha. Overall, 242.90 ha, or 12.4% of Bukik Batabuah, experienced a change in NDVI class.

Table 2. Changes in NDVI Classes Before and After the Disaster

Study area	NDVI class	Pre-disaster (ha)	Post-disaster (ha)	Change (ha)
Sungai Pua	Non-vegetated land	23.35	53.12	+29.77
	Very low vegetation	29.90	65.94	+36.04
	Low vegetation	112.92	196.31	+83.39
	Moderate vegetation	505.13	579.05	+73.92
	High vegetation	799.02	575.90	−223.12
Bukik Batabuah	Non-vegetated land	2.37	9.13	+6.76
	Very low vegetation	6.43	20.47	+14.04
	Low vegetation	50.21	84.89	+34.68
	Moderate vegetation	442.07	508.02	+65.95
	High vegetation	1,465.01	1,343.58	−121.43

Source: Sentinel-2 image processing, 2026.

The spatial expression of these changes is presented in Figure 2, NDVI Maps Before and After the Disaster in Sungai Pua and Bukik Batabuah. Comparison of the pre- and post-disaster maps shows a visible contraction of areas characterized by high NDVI values, particularly along locations affected by the lahar flow. Sungai Pua displayed a stronger shift from high vegetation toward lower vegetation and non-vegetated surface classes than Bukik Batabuah.

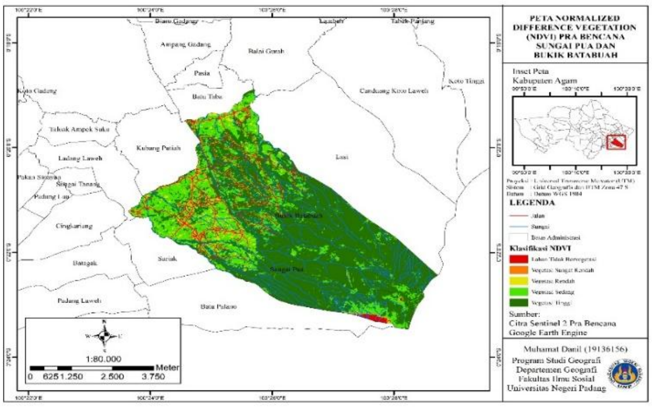

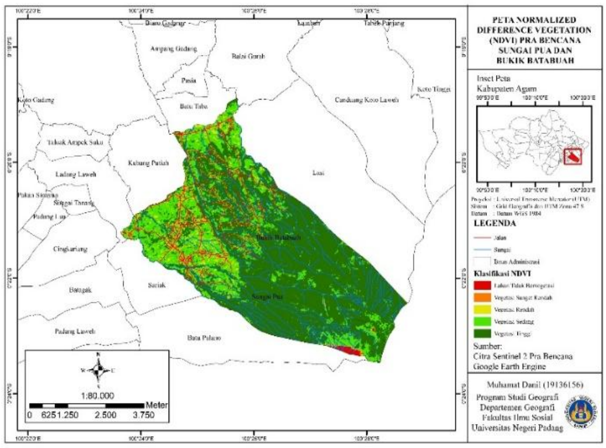

Figure 2. NDVI Maps Before and After the Disaster in Sungai Pua and Bukik Batabuah

The contrast between the two areas is particularly evident in the decline of high vegetation. Sungai Pua recorded a 15.2% reduction, compared with 6.2% in Bukik Batabuah. The spatial and quantitative results therefore indicate that vegetation disturbance following the May 2024 lahar event was more pronounced in Sungai Pua.

b. NDBI Changes

The *Normalized Difference Built-up Index* (NDBI) was used to examine changes in built-up and non-vegetated surface characteristics. The results indicate substantial post-disaster modification in both areas, although the proportional change was greater in Sungai Pua.

Table 3 shows that dense vegetation represented by the lowest NDBI class in Sungai Pua decreased from 597.34 ha to 269.54 ha, a reduction of 327.80 ha. Moderate vegetation increased by 150.41 ha, while bare land and low built-up areas increased by 90.43 ha. Moderate built-up areas increased by 22.00 ha, and the class categorized as dense built-up surface increased from 19.51 ha to 84.47 ha. Taken together, changes among NDBI classes covered approximately 655.60 ha or 44.6% of Sungai Pua.

Bukik Batabuah also showed a decline in the dense vegetation class, from 1,210.24 ha to 882.48 ha, or 327.76 ha. Moderate vegetation increased by 244.80 ha, bare land and low built-up areas by 51.10 ha, moderate built-up areas by 26.06 ha, and dense built-up areas by 5.80 ha. Total changes among NDBI classes accounted for approximately 655.52 ha or 33.3% of the area.

Table 3. Changes in NDBI Classes Before and After the Disaster

Study area	NDBI class	Pre-disaster (ha)	Post-disaster (ha)	Change (ha)
Sungai Pua	Dense vegetation	597.34	269.54	−327.80
	Moderate vegetation	665.13	815.54	+150.41
	Bare land/low built-up area	101.27	191.70	+90.43
	Moderate built-up area	87.07	109.07	+22.00
	Dense built-up area	19.51	84.47	+64.96
Bukik Batabuah	Dense vegetation	1,210.24	882.48	−327.76
	Moderate vegetation	698.84	943.64	+244.80
	Bare land/low built-up area	36.65	87.75	+51.10
	Moderate built-up area	17.26	43.32	+26.06
	Dense built-up area	3.10	8.90	+5.80

Source: Sentinel-2 image processing, 2026.

Figure 3, NDBI Maps Before and After the Disaster in Sungai Pua and Bukik Batabuah, illustrates the spatial distribution of these surface changes. Sungai Pua exhibited a larger proportional change in NDBI classes, at 44.6%, compared with 33.3% in Bukik Batabuah. Although the absolute changed areas were almost identical, their proportions differed because Sungai Pua has a smaller administrative area.

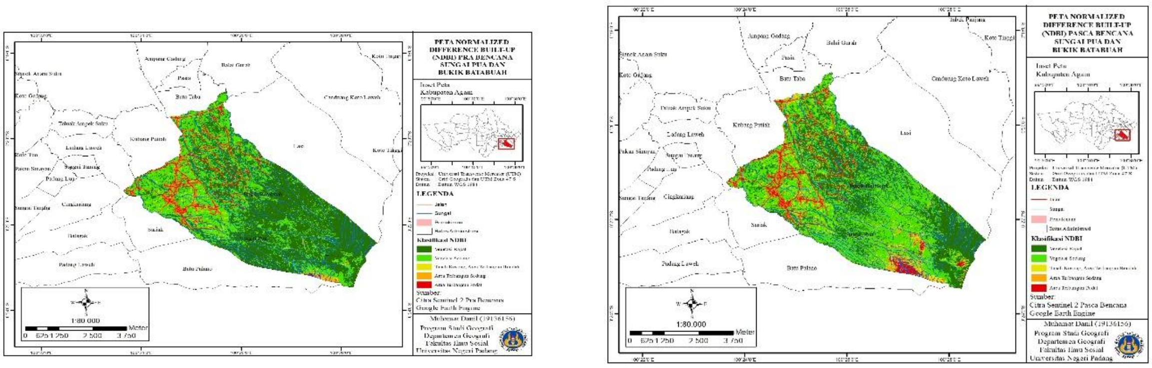

Figure 3. NDBI Maps Before and After the Disaster in Sungai Pua and Bukik Batabuah

3. **Change Detection and Residential Damage**

a. Changes in ΔNDVI and ΔNDBI

Change detection was performed by calculating differences between pre- and post-disaster spectral indices. Positive ΔNDVI and ΔNDBI values were used to identify areas showing progressively greater changes in vegetation and built-up surface characteristics.

The ΔNDVI classification presented in **Table 4** shows that 975.41 ha or 66.3% of Sungai Pua was categorized within the three damaged classes. This consisted of 532.93 ha classified as lightly damaged, 284.67 ha as moderately damaged, and 157.81 ha as severely damaged. Bukik Batabuah contained a larger absolute affected area of 1,080.25 ha, or approximately 54.9% of its total area, including 765.48 ha of light damage, 244.33 ha of moderate damage, and 70.44 ha of severe damage.

Table 4. ΔNDVI-Based Change Classification

Classification	ΔNDVI	Sungai Pua (ha)	Sungai Pua (%)	Bukik Batabuah (ha)	Bukik Batabuah (%)
Vegetation increase	< −0.10	133.14	9.1	131.97	6.7
No damage	−0.10–0.00	361.77	24.6	753.87	38.3
Light damage	0.00–0.10	532.93	36.2	765.48	39.0
Moderate damage	0.10–0.30	284.67	19.4	244.33	12.4
Severe damage	>0.30	157.81	10.7	70.44	3.6
Total	—	1,470.32	100.0	1,966.09	100.0

Source: Sentinel-2 image processing, 2026.

Although Bukik Batabuah had the larger total area categorized as affected, the proportion of severe ΔNDVI change was considerably higher in Sungai Pua. Severe change accounted for 10.7% of Sungai Pua but only 3.6% of Bukik Batabuah. This spatial pattern was consistent with field observations in Kapalo Koto and Galuang, where several residential areas were located close to the lahar-flow corridor.

The ΔNDBI analysis produced a more specific representation of change in built-up surface characteristics. As shown in **Table 5**, the combined lightly, moderately, and severely damaged classes covered 464.89 ha or 31.6% of Sungai Pua. Light damage represented 374.85 ha, moderate damage 75.73 ha, and severe damage 14.31 ha. Bukik Batabuah recorded 655.08 ha or 33.3% across the three damage classes, including 576.93 ha of light damage, 66.90 ha of moderate damage, and 11.25 ha of severe damage.

Table 5. ΔNDBI-Based Change Classification

Classification	ΔNDBI	Sungai Pua (ha)	Sungai Pua (%)	Bukik Batabuah (ha)	Bukik Batabuah (%)
Increase in built-up characteristics	< −0.10	486.54	33.1	439.19	22.3
No damage	−0.10–0.00	518.89	35.2	871.82	44.4
Light damage	0.00–0.10	374.85	25.5	576.93	29.3
Moderate damage	0.10–0.20	75.73	5.2	66.90	3.4
Severe damage	>0.20	14.31	1.0	11.25	0.6
Total	—	1,470.32	100.0	1,966.09	100.0

Source: Sentinel-2 image processing, 2026.

The smaller affected area detected by ΔNDBI than by ΔNDVI reflects the smaller proportion of built-up land relative to vegetation across both study areas. The results nevertheless reveal measurable changes in surfaces associated with residential and other built environments following the disaster.

b. Post-Classification Comparison of Land Cover

A *Post-Classification Comparison* (PCC) was conducted using land-cover maps independently classified through the *Maximum Likelihood Classification* method. Five land-cover classes were identified: built-up/residential area, vegetation, water bodies or rivers, open land/volcanic material, and agricultural land.

Figure 4, Land-Cover Maps Before and After the Disaster, shows that pre-disaster land cover was dominated by vegetation and agricultural land. Built-up areas generally followed the road network, while water bodies corresponded mainly to river corridors originating on Mount Marapi. Open land and exposed volcanic material occupied comparatively limited areas before the event. The post-disaster map shows a conspicuous expansion of open land and volcanic deposits along affected corridors, accompanied by reductions in vegetation and changes in some residential areas.

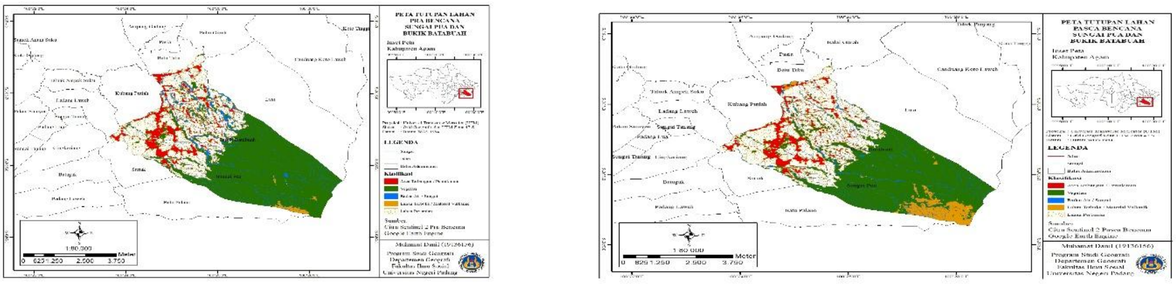

Figure 4. Land-Cover Maps Before and After the Disaster in Sungai Pua and Bukik Batabuah

Changes in land-cover area are summarized in **Table 6**. Sungai Pua experienced a decline of 4.71 ha in built-up/residential land and 177.01 ha in vegetation. Open land and volcanic material increased markedly from 31.97 ha to 208.67 ha, representing an expansion of 176.70 ha. The similarity between the decline in vegetation and increase in exposed volcanic material indicates a substantial transformation of previously vegetated surfaces within affected areas.

Bukik Batabuah showed a different pattern. Built-up/residential land declined from 95.39 ha to 71.87 ha, representing a loss of 23.52 ha. Open land and volcanic material increased by 19.98 ha, while the mapped water-body class decreased by 79.54 ha. Agricultural land increased by 84.29 ha in the post-disaster classification.

Table 6. Land-Cover Changes Based on Post-Classification Comparison

Study area	Land-cover class	Pre-disaster (ha)	Post-disaster (ha)	Net change (ha)
Sungai Pua	Built-up/residential	156.79	152.08	−4.71
	Vegetation	771.78	594.77	−177.01
	Water body/river	0.02	3.20	+3.18
	Open land/volcanic material	31.97	208.67	+176.70
	Agricultural land	509.76	511.60	+1.84
Bukik Batabuah	Built-up/residential	95.39	71.87	−23.52
	Vegetation	1,047.93	1,046.72	−1.21
	Water body/river	120.44	40.90	−79.54
	Open land/volcanic material	0.39	20.37	+19.98
	Agricultural land	701.94	786.23	+84.29

Source: Maximum Likelihood Classification of Sentinel-2 imagery, 2026.

Across the two study areas, the built-up/residential class decreased by a combined 28.23 ha, whereas open land and volcanic material increased by 196.68 ha. The largest increase occurred in Sungai Pua, where exposed volcanic material expanded by 176.70 ha. These results indicate that the physical footprint of the lahar was not confined to residential land but extended considerably across vegetation and other surfaces bordering the flow corridors.

4. Field-Validated Residential Damage

Field surveys were conducted to verify the spatial interpretation obtained from satellite imagery and to document the actual condition of residential buildings affected by the 11 May 2024 lahar event. A total of **114 damaged residential buildings** were identified: 65 in Nagari Sungai Pua and 49 in Nagari Bukik Batabuah. Each building was georeferenced using GPS and classified as lightly, moderately, or severely damaged based on direct observations of structural conditions, including damage to foundations, walls, and roofs, as well as the accumulation of volcanic material.

Figure 5, Residential Damage Maps of Sungai Pua and Bukik Batabuah, presents the locations and severity classes obtained through the field survey. In Sungai Pua, damage was distributed across Jorong Galuang and Jorong Kapalo Koto. In Bukik Batabuah, the affected buildings were concentrated in Jorong Batabuah Koto Baru.

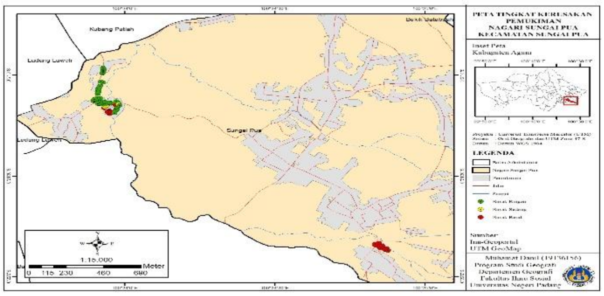

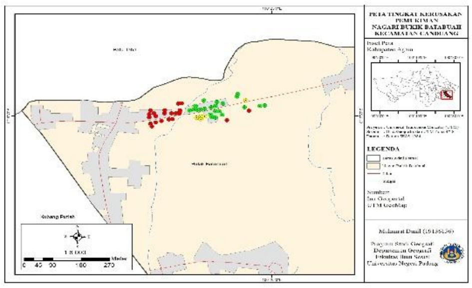

Figure 5. Residential Damage Maps of Sungai Pua and Bukik Batabuah

The field-survey results are presented in **Table 7**. Jorong Galuang had the largest number of documented damaged buildings, with 54 units. Most were lightly damaged (42 units), while four were moderately damaged and eight were severely damaged. Jorong Kapalo Koto contained only 11 documented damaged buildings, but all 11 were classified as severely damaged. Jorong Batabuah Koto Baru contained 49 affected buildings, consisting of 22 lightly damaged, five moderately damaged, and 22 severely damaged units.

Table 7. Residential Damage Identified through Field Survey

District	Location	Light	Moderate	Severe	Total
Sungai Pua	Jorong Galuang, Nagari Sungai Pua	42	4	8	54
Sungai Pua	Jorong Kapalo Koto, Nagari Sungai Pua	0	0	11	11
Canduang	Jorong Batabuah Koto Baru, Nagari Bukik Batabuah	22	5	22	49
Total		64	9	41	114

Source: Field survey and GPS tracking, 2026.

Overall, light damage was recorded in 64 buildings, moderate damage in nine buildings, and severe damage in 41 buildings. The distribution was not uniform across locations. Galuang was dominated by light damage, Kapalo Koto consisted entirely of severely damaged buildings, and Batabuah Koto Baru displayed an almost equal number of lightly and severely damaged buildings. These variations provide direct field evidence that the severity of residential damage differed substantially within and between the two study areas.

5. Spatial Pattern of Residential Damage

a. Hazard Zones Based on Distance from Lahar Channels

The spatial relationship between residential areas and lahar-flow channels was examined by establishing distance-based buffer zones around Batang Aia Lurah and Batang Aia Silasiah. Three hazard zones were defined: high hazard within 0–300 m, moderate hazard within 300–400 m, and low hazard within 400–500 m.

As shown in **Table 8**, the high-hazard zone occupied the largest area in both locations. In Sungai Pua, 384.83 ha fell within 300 m of the lahar channel, compared with 89.83 ha in the moderate zone and 83.71 ha in the low-hazard zone. Bukik Batabuah contained 322.16 ha in the high-hazard zone, 96.14 ha in the moderate zone, and 94.11 ha in the low-hazard zone.

Table 8. Hazard Zones Based on Distance from Lahar-Flow Channels

Hazard level	Distance (m)	Score	Sungai Pua (ha)	Bukik Batabuah (ha)
High	0–300	3	384.83	322.16
Moderate	300–400	2	89.83	96.14
Low	400–500	1	83.71	94.11
Total			558.38	512.41

Source: Spatial data processing, 2026.

The larger extent of the high-hazard buffer in Sungai Pua indicates that a greater portion of the analyzed area lies close to the identified lahar-flow corridor. This spatial configuration is consistent with the concentration of documented damage in settlements located near the river system.

b. Ripley's K-Function Analysis

The spatial pattern of residential damage was evaluated using *Multi-Distance Spatial Cluster Analysis (Ripley's K-function)*. The 114 field-verified damage points were analyzed separately for Sungai Pua and Bukik Batabuah because the two areas displayed different spatial configurations.

Figure 6, Spatial Distribution of Residential Damage in Sungai Pua and Bukik Batabuah, shows the contrasting organization of damaged buildings. Sungai Pua contained two identifiable concentrations corresponding to Galuang and Kapalo Koto, whereas the damaged buildings in Bukik Batabuah were distributed within the Batabuah Koto Baru area.

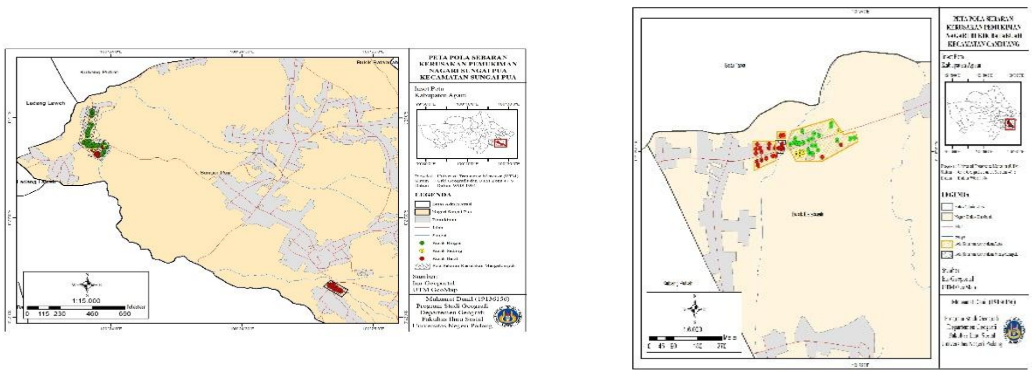

Figure 6. Spatial Distribution of Residential Damage in Sungai Pua and Bukik Batabuah

For Sungai Pua, Ripley's K-function was calculated over ten distance bands ranging from 60 to 600 m at 60-m increments. The results are shown in **Table 9**. The *Observed K* value exceeded the upper confidence envelope at every tested distance. At 60 m, for example, *Observed K* reached 216.72, substantially higher than the upper confidence limit of 75.64. This relationship persisted throughout all distance bands, demonstrating a statistically identifiable clustered pattern from 60 to 600 m.

Table 9. Ripley's K-Function Results for Sungai Pua

Distance (m)	Expected K	Observed K	Lower confidence envelope	Upper confidence envelope	Pattern
60	60.00	216.72	46.20	75.64	Clustered
120	120.00	341.81	108.86	134.35	Clustered
180	180.00	408.23	166.95	204.37	Clustered

Distance (m)	Expected K	Observed K	Lower confidence envelope	Upper confidence envelope	Pattern
240	240.00	447.29	226.17	273.82	Clustered
300	300.00	482.14	269.48	320.77	Clustered
360	360.00	514.85	311.18	370.62	Clustered
420	420.00	532.43	347.60	410.98	Clustered
480	480.00	532.75	375.01	445.25	Clustered
540	540.00	532.75	404.25	481.72	Clustered
600	600.00	532.75	427.48	510.83	Clustered

Source: Multi-Distance Spatial Cluster Analysis, ArcGIS, 2026.

The curve presented in Figure 7a, Ripley's K-Function for Sungai Pua, confirms this result visually. The observed function remains above the upper confidence envelope throughout the analyzed range. The *Observed K* value becomes constant at 532.75 from approximately 480 m onward, indicating that additional increases in distance no longer substantially change the number of point relationships captured within the analysis.

Bukik Batabuah produced a distinctly different pattern. The analysis used ten distance bands from 10 to 100 m at 10-m increments. As shown in **Table 10**, the *Observed K* value remained within the confidence envelope at nine of the ten tested distances. At 10, 20, 30, and 40 m, the observed values did not exceed the upper confidence limit. A localized departure occurred at 50 m, where *Observed K* reached 55.08 compared with an upper confidence envelope of 53.58. At distances from 60 to 100 m, the observed values returned to within the confidence envelope.

Table 10. Ripley's K-Function Results for Bukik Batabuah

Distance (m)	Expected K	Observed K	Lower confidence envelope	Upper confidence envelope	Pattern
10	10.00	11.07	5.46	13.83	Random
20	20.00	22.38	15.96	23.00	Random
30	30.00	31.25	24.89	33.34	Random
40	40.00	43.73	36.55	45.98	Random
50	50.00	55.08	46.36	53.58	Clustered
60	60.00	63.27	54.68	65.76	Random
70	70.00	72.39	64.23	76.54	Random
80	80.00	80.42	70.59	84.55	Random
90	90.00	87.80	78.84	93.67	Random
100	100.00	95.18	87.64	100.24	Random

Source: Multi-Distance Spatial Cluster Analysis, ArcGIS, 2026.

Figure 7b, Ripley's K-Function for Bukik Batabuah, shows that the observed curve generally follows the range expected under *Complete Spatial Randomness* (CSR). The only statistically identifiable local clustering occurred at the 50-m distance band. The pattern therefore differs from Sungai Pua, where clustering was consistently observed across all tested distances.

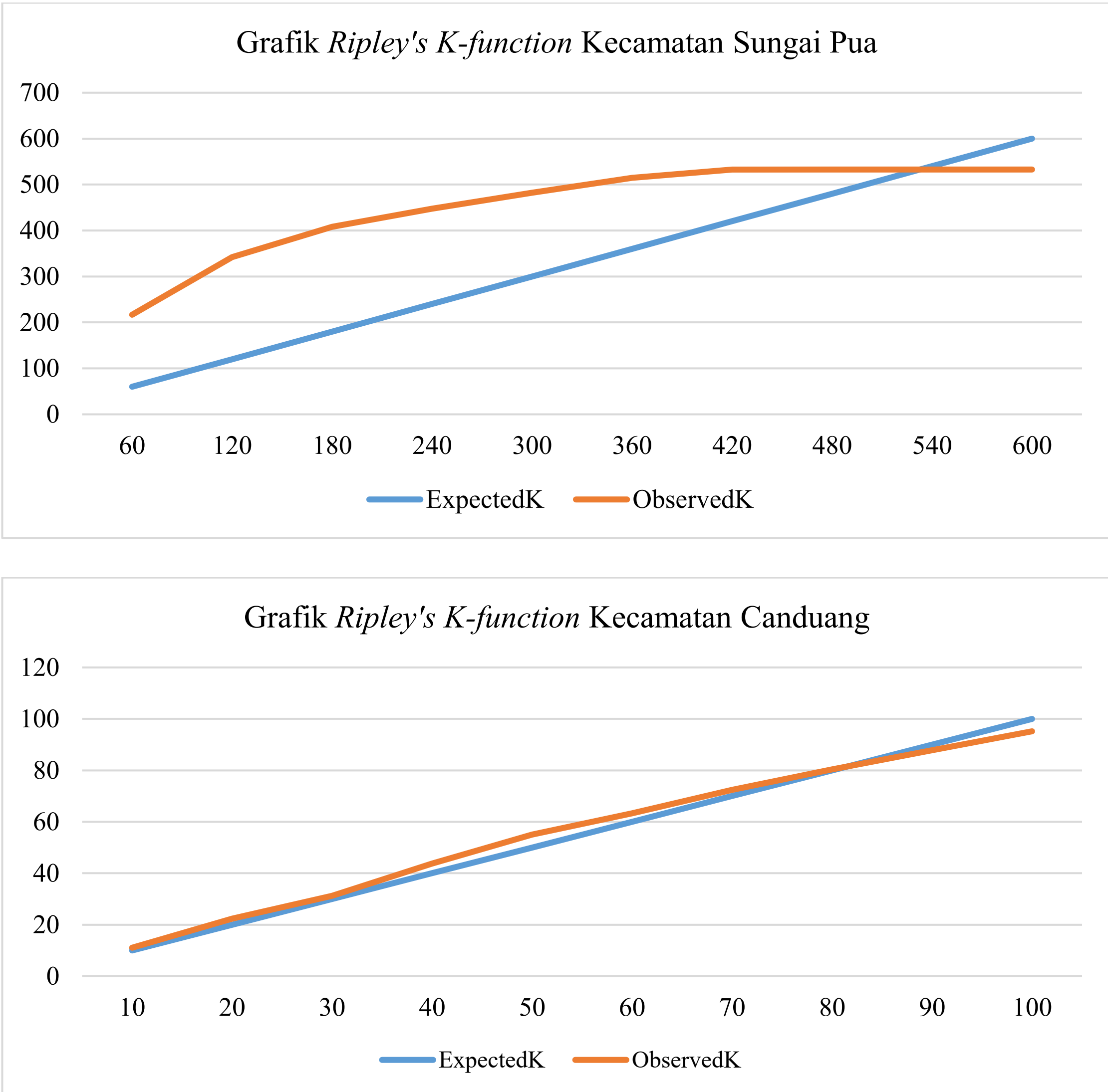

Figure 7. Ripley's K-Function Graphs for (a) Sungai Pua and (b) Bukik Batabuah

Taken together, the spatial analyses reveal two different configurations of residential damage. Sungai Pua exhibited a consistently clustered pattern from 60 to 600 m, corresponding spatially with concentrations of damaged buildings in Galuang and Kapalo Koto. Bukik Batabuah generally exhibited a random spatial pattern from 10 to 100 m, with a localized clustering tendency only at 50 m. The field survey, distance-based hazard zoning, and Ripley's K-function results therefore consistently demonstrate that residential damage was spatially more concentrated in Sungai Pua, whereas damage in Bukik Batabuah was comparatively less organized into persistent clusters across the tested distance scales.

DISCUSSION

1. Residential Damage Based on Change Detection

The integration of spectral-index analysis, *Post-Classification Comparison* (PCC), and field verification provides consistent evidence that the 11 May 2024 Mount Marapi cold lahar flood produced measurable changes in both the physical landscape and residential areas of Sungai Pua and Bukik Batabuah. The use of several analytical components is particularly important because disaster-related surface change cannot be represented adequately by a single spectral indicator. Changes in NDVI primarily reflect the loss or modification of vegetation cover, whereas NDBI provides additional information on built-up and exposed surfaces. PCC complements these continuous spectral measures by identifying categorical transitions between pre- and post-disaster land-cover classes. This combined approach is consistent with remote-sensing studies showing that multi-temporal and multi-indicator analysis improves the interpretation of disaster-induced surface change compared with reliance on a single image or index (Goswami et al., 2022; Mei et al., 2023; Zakeri et al., 2019). It also responds to the concern that post-classification approaches remain sensitive to classification errors generated independently at each observation period, making field verification an important component of damage interpretation.

The results indicate that Sungai Pua experienced proportionally more intensive landscape disturbance than Bukik Batabuah. High-density vegetation declined by 15.2% in Sungai Pua compared with 6.2% in Bukik Batabuah, while severely changed areas based on ΔNDVI accounted for 10.7% and 3.6%, respectively. Although Bukik Batabuah contained a larger absolute area classified as affected, this difference should be interpreted in relation to its larger administrative area. The proportional results therefore provide a clearer indication of relative disturbance intensity. The pattern is also compatible with the physical setting of the study area. Settlements in Galuang and Kapalo Koto are associated with the Batang Aia Lurah corridor, where the movement of water, sediment, and coarse volcanic material can concentrate destructive energy within relatively narrow pathways. Studies of rain-triggered lahars have similarly shown that flow behavior and destructive capacity are strongly influenced by channel configuration, sediment concentration, and the spatial relationship between flow paths and exposed elements (Ramos et al., 2024; Tierz et al., 2024). The observed damage should consequently be understood as the outcome of an interaction between volcanic material, topography, river corridors, and the location of settlements rather than as a simple consequence of inundation alone.

The field survey provides a more direct representation of how these spatial processes affected individual buildings. Of the 114 documented damaged houses, 41 were severely damaged, nine were moderately damaged, and 64 were lightly damaged. The most striking local pattern occurred in Kapalo Koto, where all 11 documented houses were classified as severely damaged. Galuang displayed a more varied profile, with 42 lightly damaged, four moderately damaged, and eight severely damaged houses. Bukik Batabuah showed a different distribution, with 22 lightly damaged and 22 severely damaged houses, accompanied by five moderately damaged units. These differences also explain why pixel-based spectral analysis and building-level observations do not necessarily produce identical proportions of damage. Spectral indices describe changes across surface pixels, including vegetation, exposed ground, volcanic deposits, and built-up land, whereas the field survey evaluates individual residential structures. The two scales therefore capture different dimensions of the same disaster. Their convergence strengthens the interpretation of the affected landscape, while their differences caution against treating spectral change as a direct substitute for structural damage assessment.

The land-cover comparison further illustrates this distinction. Sungai Pua recorded a 176.70 ha increase in open land and volcanic material, closely accompanied by a 177.01 ha reduction in vegetation. This near correspondence suggests that a substantial portion of the post-disaster landscape transformation involved the replacement or burial of previously vegetated surfaces by exposed volcanic deposits. Bukik Batabuah experienced a smaller increase in open land and volcanic material, although its built-up/residential class declined by 23.52 ha. Similar applications of satellite imagery have demonstrated that disaster-induced transitions can be detected through changes in spectral properties and land-cover categories, particularly when pre- and post-event imagery is available (Braik & Koliou, 2024). In the Mount Marapi context, Sari & Triyatno (2024) also demonstrated the usefulness of Sentinel-2 imagery for identifying areas affected by cold lahar in Sungai Pua. The present study extends that spatial perspective by combining NDVI, NDBI, PCC, and building-level *ground* *checks*, allowing the effects on vegetation, built-up surfaces, land-cover classes, and individual houses to be considered together rather than separately.

The findings are also consistent with earlier studies of the Mount Marapi disaster that emphasize the spatial concentration of risk around lahar pathways. Aisy and Hermon (2025) identified substantial lahar hazard and risk through GIS-based scoring and overlay analysis, while Yanto et al. (2024) documented damage to settlement land in areas affected by the same volcanic system. Wulandari et al. (2025) further highlighted the importance of spatial considerations in identifying evacuation locations on the southern side of Mount Marapi. The present findings add a different layer to this body of evidence. Rather than focusing only on generalized hazard or affected-area delineation, the analysis demonstrates that the intensity and form of damage differ between nearby settlements exposed to the same regional disaster. This distinction is important for post-disaster planning because two areas classified within a similar hazard environment may still exhibit substantially different patterns of structural and landscape damage.

2. Spatial Pattern of Residential Damage

The Ripley's K-function analysis reveals a marked contrast between Sungai Pua and Bukik Batabuah. In Sungai Pua, the *Observed K* value exceeded the upper confidence envelope at all ten tested distance bands from 60 to 600 m. The difference was particularly pronounced at 60 m, where the *Observed K* value reached 216.72 compared with an upper confidence limit of 75.64. The persistence of this relationship across the entire analyzed range indicates that residential damage was not randomly distributed but formed a strong and spatially consistent clustered pattern. The stabilization of *Observed K* at 532.75 from approximately 480 m onward indicates that increasing the search distance beyond this scale added little to the number of spatial relationships represented in the analysis. Such a pattern corresponds well with field observations showing two concentrations of damaged buildings in Galuang and Kapalo Koto. Ripley's K-function is particularly useful in this context because it examines spatial dependence across several distances rather than describing clustering at only one scale (Self et al., 2023; Vidanapathirana et al., 2022).

Bukik Batabuah exhibited a substantially different spatial structure. Nine of the ten tested distance bands remained within the confidence envelope expected under *Complete Spatial Randomness*, while statistically identifiable clustering occurred only at 50 m. The localized departure at this distance most likely reflects the immediate proximity of neighboring damaged houses within Jorong Batabuah Koto Baru rather than a persistent multi-scale clustering pattern. The return of the observed values to the confidence envelope at distances above 50 m indicates that this local concentration does not extend consistently across the wider spatial range. This result demonstrates the value of multi-distance analysis: an area may contain visually recognizable concentrations of damaged houses without displaying statistically persistent clustering at broader scales. Self et al. (2023) similarly emphasize that spatial clustering may vary with distance and that conclusions based on a single spatial scale can obscure important changes in spatial structure.

Distance-based hazard zoning provides complementary evidence but should not be interpreted as equivalent to the Ripley's K-function results. High-hazard zones within 300 m of the lahar channels represented approximately 68.9% of the analyzed buffer area in Sungai Pua and 62.9% in Bukik Batabuah. Both areas therefore contained substantial land close to the identified flow corridors, yet their observed residential-damage patterns differed. Sungai Pua showed persistent clustering, whereas Bukik Batabuah was predominantly consistent with spatial randomness. This contrast suggests that distance from the river is important but does not independently determine the final spatial organization of damage. Settlement configuration, building density, local channel morphology, flow direction, and the distribution of volcanic deposits may alter how exposure translates into actual structural damage. The finding supports the broader argument that GIS-based hazard analysis benefits from combining proximity measures with observed-event data rather than assuming that equal distances from a hazard source necessarily produce equal patterns of damage.

The use of Ripley's K-function also contributes methodologically to disaster-damage assessment. Previous applications have demonstrated the usefulness of the method for identifying distance-dependent spatial organization across different geographical phenomena (Self et al., 2023; Zhang & Zhang, 2025). Its application to lahar-related residential damage in this study shows that the same analytical framework can distinguish persistent clustering from local or essentially random distributions of damaged buildings. The practical value lies in identifying the spatial scales at which damage concentration becomes evident. For disaster management, a consistently clustered pattern such as that observed in Sungai Pua may indicate locations where mitigation, relocation assessment, evacuation planning, and infrastructure protection should be considered as interconnected spatial interventions rather than as isolated building-level responses.

3. Implications and Research Limitations

The combined findings have practical implications for post-disaster assessment and future risk reduction around Mount Marapi. GIS and multi-temporal remote sensing provide a means of rapidly identifying broad landscape changes, while field verification supplies the structural detail required to distinguish the actual severity of residential damage. Combining these sources is therefore more informative than relying exclusively on satellite-derived indices or field observations. The resulting information can support the prioritization of rehabilitation, identification of residential areas requiring closer monitoring, and development of settlement planning that considers both lahar-flow corridors and the spatial concentration of previously damaged buildings. The contrast between Sungai Pua and Bukik Batabuah also indicates that mitigation strategies should be adapted to local spatial conditions rather than applied uniformly across neighboring districts.

Several limitations should nevertheless be considered when interpreting the findings. Sentinel-2 imagery is suitable for landscape-scale change detection, but its spatial resolution limits the identification of detailed structural damage to individual houses. Spectral changes may also reflect mixtures of volcanic deposits, vegetation loss, exposed soil, moisture, and built surfaces, meaning that changes in NDVI or NDBI should not automatically be interpreted as direct building damage. PCC is influenced by the accuracy of the independent pre- and post-disaster classifications, while the field survey records building conditions observed after the event without reconstructing every intermediate stage of damage. The Ripley's K-function analyses were also performed using different distance ranges in Sungai Pua and Bukik Batabuah because of their different point configurations, which requires caution when comparing the magnitude of K-values directly between the two areas. Future research could strengthen the analysis by incorporating higher-resolution imagery, building materials and structural characteristics, detailed flow-depth or sediment-thickness measurements, and standardized distance parameters where spatial conditions allow. These additions would help explain not only where damage occurs, but also why buildings exposed to apparently similar lahar environments experience different levels of destruction.

CONCLUSION

Based on the research findings and discussion, the application of Geographic Information Systems (GIS) combined with *change detection* analysis successfully identified the extent and spatial characteristics of residential damage caused by the 11 May 2024 Mount Marapi cold lahar flood in Sungai Pua and Canduang Districts. The ΔNDVI analysis showed that affected areas reached 975.41 ha (66.3%) in Nagari Sungai Pua and 1,080.25 ha (54.9%) in Nagari Bukik Batabuah, while the ΔNDBI analysis identified 464.89 ha (31.6%) and 655.08 ha (33.3%) of affected areas, respectively. The *Post-Classification Comparison* also revealed a substantial expansion of open land and volcanic material, particularly in Sungai Pua, where this class increased by 176.70 ha, compared with 19.98 ha in Bukik Batabuah. Field verification documented 114 damaged residential buildings, consisting of 64 lightly damaged, nine moderately damaged, and 41 severely damaged units. These findings show that satellite-based spectral analysis and field observations provide complementary information for understanding both landscape-scale change and building-level damage.

The spatial analysis further revealed different patterns of residential damage between the two study areas. Sungai Pua exhibited a significant clustered pattern across all tested distances from 60 to 600 m, whereas Bukik Batabuah generally followed *Complete Spatial Randomness*, with localized clustering identified only at 50 m. High-hazard zones within 0–300 m of the lahar channels also dominated both areas, covering 68.9% of the analyzed zone in Sungai Pua and 62.9% in Bukik Batabuah. These results indicate that residential damage is shaped not only by proximity to lahar-flow channels but also by local topography, settlement configuration, and the spatial concentration of exposed buildings. The findings may support local governments and disaster management agencies in strengthening risk-sensitive spatial planning, evaluating settlements located near lahar corridors, and improving rainfall- and river-discharge-based early warning systems. Future studies are recommended to integrate higher-resolution satellite imagery, building construction characteristics, sediment depth, and more detailed flow parameters to provide a more precise assessment of residential vulnerability to future lahar events.

REFERENCES

Aisy, R., & Hermon, D. (2024). Tingkat Bahaya dan Risiko Bencana Banjir Lahar Dingin Gunung Marapi Berbasis Sistem Informasi Geografis (SIG) Menggunakan Metode

Skoring dan Overlay di Kabupaten Tanah Datar. *Jurnal Pendidikan Tambusai, 8*(2), 18859–18873. https://doi.org/10.31004/jptam.v8i2.15152

Azizah, V., & Irawan, L. Y. (2023). Deteksi Perubahan Jalur Lahar di Curah Lengkong Pascaerupsi Gunungapi Semeru 2021 Menggunakan Google Earth Engine. *Jurnal Geografi, Edukasi dan Lingkungan (JGEL), 7*(1), 70–93. https://doi.org/10.22236/jgel.v7i1.10321

Badan Nasional Penanggulangan Bencana. (2024, May 12). *[Update] Korban Meninggal Pascabanjir Bandang Agam Jadi 19 Orang*. https://bnpb.go.id/berita/update-korban-meninggal-pascabanjir-bandang-agam-jadi-19-orang

Badan Penanggulangan Bencana Daerah Kabupaten Agam. (2024). *Laporan Dampak Bencana Banjir Lahar Dingin Gunung Marapi Tanggal 11 Mei 2024*.

Braik, A. M., & Koliou, M. (2024). Automated building damage assessment and large-scale mapping by integrating satellite imagery, GIS, and deep learning. *Computer-Aided Civil and Infrastructure Engineering, 39*(15), 2389–2404. https://doi.org/10.1111/mice.13197

Budiarto, F. A., & Bioresita, F. (2023). Pemanfaatan Citra Sentinel-1 SAR dan Metode Change Detection Approach untuk Analisis Sebaran Spasial Wilayah Banjir dan Area Terdampak (Studi Kasus: Banjir Kabupaten Aceh Utara 2022). *JGISE: Journal of Geospatial Information Science and Engineering, 6*(2), 153–162. https://doi.org/10.22146/jgise.87585

Goswami, A., Sharma, D., Mathuku, H., Gangadharan, S. M. P., Yadav, C. S., Sahu, S. K., Pradhan, M. K., Singh, J., & Imran, H. (2022). Change detection in remote sensing image data comparing algebraic and machine learning methods. *Electronics, 11*(3), 431. https://doi.org/10.3390/electronics11030431

Hermon, D. (2015). *Geografi Bencana Alam*. Rajawali Pers.

Mei, J., Zheng, Y.-B., & Cheng, M.-M. (2023). D2ANet: Difference-aware attention network for multi-level change detection from satellite imagery. *Computational Visual Media, 9*(3), 563–579. https://doi.org/10.1007/s41095-022-0325-1

Sari, K. Y., & Triyatno. (2024). Analisis Bencana Banjir Menggunakan Data SAR (Synthetic Aperture Radar) Sentinel-1 di Kecamatan Sungai Serut Kota Bengkulu. *MASALIQ: Jurnal Pendidikan dan Sains, 4*(3), 722–741. https://doi.org/10.58578/masaliq.v4i3.3045

Sari, R. P., Arini, D., Driptufany, D. M., Fajrin, & Armi, I. (2025). Pemetaan Kawasan Terdampak Akibat Lahar Dingin Gunung Marapi dan Sekitarnya Menggunakan Citra Satelit Sentinel-2 (Studi Kasus: Kecamatan Sungai Pua, Kabupaten Agam). *Jurnal Sains dan Ilmu Terapan, 8*(2), 50–60. https://doi.org/10.59061/jsit.v8i2.1210

Self, S., Overby, A., Zgodic, A., White, D., McLain, A. C., & Dyckman, C. (2023). A hypothesis test for detecting distance-specific clustering and dispersion in areal data. *Spatial Statistics, 55*, 100757. https://doi.org/10.1016/j.spasta.2023.100757

Vidanapathirana, N., Wang, Y., McLain, A. C., & Self, S. (2022). *Cluster detection capabilities of the average nearest neighbor ratio and Ripley's K function on areal data: An empirical assessment* [Preprint]. arXiv. https://doi.org/10.48550/arXiv.2204.10882

Wulandari, F., Edial, H., & Purwaningsih, E. (2025). Studi Lokasi Evakuasi Masyarakat dalam Mitigasi Banjir Lahar Dingin di Sisi Selatan Gunung Marapi. *Al-DYAS: Jurnal Inovasi dan Pengabdian kepada Masyarakat,* *4*(1), 531–544. https://doi.org/10.58578/aldyas.v4i1.4639

Wulansari, T., Wulandini, D. R., & Harahap, E. F. (2024). Analysis of the impact of flash floods and cold lava floods on Mount Marapi, West Sumatra 2024. *Proceeding of International Conference on Digital, Social, and Science,* *1*(1), 224–230. https://doi.org/10.62201/icodss.v1i01.166

Yanto, A., Veni, V., Rahayu, I. D., Febrianto, H., Simponi, M., & Afrianto, N. (2024). Analisis Kerusakan Lahan Pemukiman pada Kawasan Berdampak Lahar Dingin Gunung Marapi Kabupaten Tanah Datar Sumatera Barat. *Jurnal Manajemen Pendidikan, 9*(3), 427–433. https://doi.org/10.34125/jmp.v9i3.353

Zakeri, F., Huang, B., & Saradjian, M. R. (2019). Fusion of change vector analysis in posterior probability space and postclassification comparison for change detection from multispectral remote sensing data. *Remote Sensing,* *11*(13), 1511. https://doi.org/10.3390/rs11131511

Zhang, T., & Zhang, S. (2025). *Spatial pattern analysis of tourism resources in Hainan Island based on Ripley's K function* [Preprint]. Research Square. https://doi.org/10.21203/rs.3.rs-7337382/v1